

## Investigation of the mechanical properties and local structural evolution of $\text{Ti}_{60}\text{Zr}_{10}\text{Ta}_{15}\text{Si}_{15}$ bulk metallic glass during tensile deformation: a molecular dynamics study

Hui-Lung Chen<sup>1</sup>, Shin-Pon Ju<sup>2,3,\*</sup>, Tsang-Yu Wu<sup>2</sup>, Shih-Hao Liu<sup>2</sup>, Hsin-Tsung Chen<sup>4</sup>

<sup>1</sup>Department of Chemistry and Institute of Applied Chemistry, Chinese Culture University, Taipei 111, Taiwan

<sup>2</sup>Department of Mechanical and Electro-Mechanical Engineering, National Sun Yat-sen University, Kaohsiung 804, Taiwan

<sup>3</sup>Department of Medicinal and Applied Chemistry, Kaohsiung Medical University, Kaohsiung 807, Taiwan

<sup>4</sup> Department of Chemistry, Chung Yuan Christian University, Chungli District, Taoyuan City 32023, Taiwan

\*Corresponding author ([jushin-pon@mail.nsysu.edu.tw](mailto:jushin-pon@mail.nsysu.edu.tw)),

### 1. Force matching method

The force-matching method (FMM) [1] was used to determine the parameters of potential functions, which were utilized to model the interactions among Ti, Zr, Ta and Si atoms in the current study. FMM is based on the variable optimization process of an objective function, which is constructed by the summation of squares of differences between the atomic forces obtained by a potential function and the corresponding atomic forces by *ab initio* or density functional theory (DFT) calculations. The original FMM minimizes the following objective function,  $Z(\alpha)$ [2]:

$$Z(\alpha) = \left( 3 \sum_{k=1}^M N_k \right)^{-1} \sum_{k=1}^M \sum_{i=1}^{N_k} \left( F_{ki}(\alpha) - F_{ki}^0 \right)^2 \quad (11)$$

Where  $\alpha$ ,  $M$  and  $N_k$  are the entire set of potential parameters, the number of atomic configurations, and the number of atoms in a configuration  $k$ .  $F_{ki}(\alpha)$  is the force acting on atom  $i$  of the configuration  $k$ , which is computed from the potential parameters  $\alpha$ .  $F_{ki}^0$  is the corresponding referenced force calculated from the *ab initio* or density functional theory (DFT) calculation approach. Except for atomic forces of all

optimized structures, the binding energy, bulk moduli, elastic constants of crystal reference structures were also included in our object function.

Twenty-two crystal configurations including four pure element systems (Ti, Zr, Ta, Si), and binary-element systems including the binary alloys that were reported in the previous study ( $\text{Zr}_3\text{Si}_2$ [3],  $\text{ZrSi}$ [4],  $\text{ZrSi}_2$ [5],  $\text{Ta}_2\text{Si}$ [6],  $\text{Ta}_5\text{Si}_3$ [6],  $\text{TaSi}_2$ [7],  $\text{TiSi}$ [8],  $\text{TiSi}_2$ [9],  $\text{Ti}_3\text{Si}$ [10]) and alloys constructed by DFT ( $\text{Zr}_1\text{Ti}_3$ ,  $\text{Zr}_2\text{Ti}_2$ ,  $\text{Zr}_3\text{Ti}_1$ ,  $\text{Zr}_1\text{Ta}_3$ ,  $\text{Zr}_2\text{Ta}_2$ ,  $\text{Zr}_3\text{Ta}_1$ ,  $\text{Ti}_1\text{Ta}_3$ ,  $\text{Ti}_2\text{Ta}_2$ ,  $\text{Ti}_3\text{Ta}_1$ ) were used to prepare the reference data for FMM as shown in Table. S1. All required reference data were directly prepared by the DFT calculation.

For the binding energies, the Dmol3 package [11] was used, and the elastic constants and bulk moduli were prepared by the CASTEP package [12]. The generalized gradient approximation (GGA) with the parameterization of Perdew-Wang generalized-gradient approximation (PW91) [13] was used for both Dmol3 and CASTEP. For Dmol3 settings, all electron calculation with a double numeric plus polarization basis set DNP [14] was used. The energy tolerance in the self-consistent field calculations was  $2.72 \times 10^{-5}$  eV, and the energy, force and atomic displacement tolerances for the ionic step were  $2.72 \times 10^{-4}$  eV,  $5.44 \times 10^{-2}$  eV/Å and  $5.00 \times 10^{-3}$  Å. For the settings of CASTEP, the energy tolerance in the self-consistent field calculations was  $5 \times 10^{-7}$  eV/atom and the convergence conditions for the ionic step were set as  $1 \times 10^{-6}$  eV/atom for the energy change,  $2 \times 10^{-3}$  eV/Å for the force change,  $1 \times 10^{-4}$  Å for the atomic displacement, 380 eV for the plane-wave cutoff energy, and 0.024 for the k-point separations.

For Ti, Zr, Ta and Si crystal structures, Table. S2 lists the lattice constants as well as the binding energies by Dmol3 optimization calculations and from the corresponding measured data[15, 16] (also in Table. S2). It can be seen that the lattice constants and binding energies obtained by Dmol3 are very close to the experimental

values, indicating the Dmol3 setting is accurately enough to predict the binding energies and geometrical properties of the Ti-Zr-Ta-Si systems. Table. S3 illustrates the lattice constants, elastic constants, bulk moduli and shear moduli of Ti, Zr, Ta and Si unit cells after the CASTEP geometry optimization and the corresponding experimental data are also shown[15-17]. The calculated lattice constants are very close to the experimental values, which are comparable to those by the Dmol3 calculation shown in Table S1. For the mechanical properties, most calculation results are in good agreement with the experimental values except for  $C_{12}$ ,  $C_{44}$  of Zr and  $C_{12}$  of Si, which can be also found in the previous studies [18, 19]. The relative values of elastic constants do not change for the calculation results, and the CASTEP settings are regarded good enough to get the mechanical properties of Ti-Zr-Ta-Si systems for preparing the FMM reference data.

The electron density distributions of Ti, Zr, Ta, Si unit cells obtained by the Dmol3 calculations are displayed in Fig. S1 (a)-(d). The electron overlap of Si-Si pair is very apparent which indicates the covalent bonding characteristics while other pairs show the metallic features. For the same idea, the electron overlaps of Ti-Si, Zr-Si and Ta-Si pairs are also shown in Fig. S2 (a)-(c). The Ti-Si and Zr-Si pairs demonstrate the covalent bonding characteristics and Ta-Si pair shows the metallic bonding characteristics. Consequently, the tight-binding potential [20] was adopted to model the metallic bonding of Ti-Ti, Zr-Zr, Ta-Ta, Ti-Zr, Ti-Ta, Zr-Ta, Ta-Si interactions and the Tersoff potential was used to describe the covalent bond interactions of Si-Si, Ti-Si and Zr-Si pairs.

### **1.1 Tight-binding potential**

Atomic interactions of Ti-Ti, Zr-Zr, Ta-Ta, Ti-Zr, Ti-Ta, Zr-Ta, Ta-Si are modeled by the many-body, tight-binding potential (TB) [17, 21-23] and the potential form is shown as Eq. (1):

$$E_i = - \left\{ \sum_j \xi^2 \exp \left[ -2q \left( \frac{r_{ij}}{r_0} - 1 \right) \right] \right\}^{1/2} + \sum_j A \exp \left[ -p \left( \frac{r_{ij}}{r_0} - 1 \right) \right] \quad (1)$$

Where  $\xi$  is an effective hopping integral,  $r_{ij}$  is the distance between atoms  $i$  and  $j$ , and  $r_0$  is the first-neighbor distance. The first part in the potential function is the summary of the band energy, which is characterized by the second moment of the d-band density of state. Meanwhile, the second part is a Born-Mayer type repulsive form. In Karolewski's studies [24], the parameters  $\xi$ ,  $A$ ,  $p$ ,  $q$ , and  $r_0$  of several transition metals were determined on the basis of the experimentally obtained values of cohesive energy, vacancy formation energy, lattice parameter and elastic constants [15, 25].

## 1.2 Tersoff potential energy

The interactions of Si-Si, Si-Ti and Si-Zr pairs are described by Tersoff potential. This potential involves both two- and three-body terms as shown below:

$$U_{total}^{Ter} = \sum_{i=1}^N E_i = \frac{1}{2} \sum_{i \neq j} V(r_{ij}) \quad (2)$$

$E_i$  is the potential energy of atom  $i$ , and the summation of  $E_i$  is the total energy.  $V(r_{ij})$  is the energy formed by atom  $i$  and atom  $j$ .  $V(r_{ij})$  is defined as:

$$V(r_{ij}) = \sum_i \sum_{j>i} f_c(r_{ij}) [f_R(r_{ij}) + b_{ij} f_A(r_{ij})] \quad (3)$$

$$f_A = -B_{ij} \exp(-u_{ij} r_{ij}) \quad (4)$$

$$f_R = A_{ij} \exp(-\lambda_{ij} r_{ij}) \quad (5)$$

The formula  $f_R$  models the repulsive interaction between atoms due to electron overlap, while  $f_A$  describes the attractive interaction associated with bonding. The

coefficient  $b_{ij}$  corresponds to a many-body interaction and the function  $f_c$  is a smooth cutoff function which limits the range of the potential. The function  $g(\theta_{ijk})$  represents the influence of the bonding angle. The formulas of these three parameters can be seen in Eqs. (6)~(8):

$$b_{ij} = (1 + \beta_i^{n_i} \zeta_{ij}^{n_i})^{-1/2n_i} \quad (6)$$

$$f_c(r_{ij}) = \begin{cases} 1, & r_{ij} < R_{ij} \\ \frac{1}{2} + \frac{1}{2} \cos[\pi \frac{(r_{ij} - R_{ij})}{(S_{ij} - R_{ij})}], & R_{ij} < r_{ij} < S_{ij} \\ 0, & S_{ij} < r_{ij} \end{cases} \quad (9)$$

$$g(\theta_{ijk}) = 1 + \frac{c_i^2}{d_i^2} - \frac{c_i^2}{[d_i^2 + (h_i - \cos \theta_{ijk})^2]} \quad (8)$$

The form of  $\zeta$  in Eq. (6) is shown below:

$$\zeta_{ij}^{n_i} = \sum_{k \neq i, j} f_c(r_{ik}) g(\theta_{ijk}) \quad (7)$$

## 2. Fitting process

Although TB parameters of Ti, Zr, Ta and Tersoff parameters of Si can be found in previous studies [17, 24, 26], these parameters were also modified by FMM to minimize the discrepancies between the reference data and the data calculated by using the fitted parameters.

For improving the many-body effect in TB potential [24], the binding energies of structures with one-atom defect were also included. During the fitting process, the object function optimization was conducted by the general utility lattice program (GULP) [27]. The idea of the basin-hopping (BB) method [28] was used to randomly change the values of TB and Tersoff parameters after each optimization process. Monte Carlo method was adopted to find the parameter set, which can obtain the global minimal value of the objective function [29]. After the fitting process, a set of

potential parameters with the accuracy comparable to the DFT calculations can be obtained, which can be seen in Table. S4 and Table. S5 for TB and Tersoff potentials, respectively. As shown in Table. S6, the reference data calculated by the TB and Tersoff potentials are compared with those by the DFT calculation. It can be seen the energy discrepancies and elastic constant discrepancies of most reference data are located within 20% and 50% , indicating the predicted material properties by TB and Tersoff potentials with our fitted parameters are in good agreement with the corresponding DFT data.

Table S1 Information of lattice constants and space group of crystalline structure  
reference data for FMM

<i>alloy</i>	<i>Space group</i>	<i>a(Å)</i>	<i>b(Å)</i>	<i>c(Å)</i>
Zr	P63/MMC	3.23	3.23	5.14
Ti	P63/MMC	2.95	2.95	4.67
Ta	IM-3M	3.30	3.30	3.30
Si	FD-3M	5.43	5.43	5.43
Zr <sub>3</sub> Ti <sub>1</sub>	PM-3M	4.43	4.43	4.43
Zr <sub>1</sub> Ti <sub>1</sub>	P4/MMM	3.06	3.06	4.10
Zr <sub>1</sub> Ti <sub>3</sub>	PM-3M	4.21	4.21	4.21
Zr <sub>3</sub> Ta <sub>1</sub>	PM-3M	4.48	4.48	4.48
Zr <sub>1</sub> Ta <sub>1</sub>	P4/MMM	2.90	2.90	5.01
Zr <sub>1</sub> Ta <sub>3</sub>	PM-3M	4.34	4.34	4.34
Ti <sub>3</sub> Ta <sub>1</sub>	PM-3M	4.14	4.14	4.14
Ti <sub>1</sub> Ta <sub>1</sub>	P4/MMM	2.81	2.81	4.64
Ti <sub>1</sub> Ta <sub>3</sub>	PM-3M	4.24	4.24	4.24
ZrSi	PNMA	7.00	3.79	5.32
ZrSi <sub>2</sub>	CMCM	3.68	14.64	3.68
Zr <sub>3</sub> Si <sub>2</sub>	P4/MBM	7.08	7.08	3.71
TiSi	PNMA	6.48	3.62	4.97
TiSi <sub>2</sub>	CMCM	3.55	13.49	3.55
Ti <sub>3</sub> Si	P42/n	10.21	10.20	5.07
Ta <sub>2</sub> Si	I4/mcm	6.25	6.25	5.17
Ta <sub>5</sub> Si <sub>3</sub>	I4/mcm	10.00	10.00	5.21
TaSi <sub>2</sub>	P6222	4.78	4.78	6.57

Table S2 Comparisons between experimental and Dmol3 DFT calculation results for hcp Zr, hcp Ti, bcc Ta and diamond structure Si. The values of a, c/a, and E are the lattice constant, the ratio for lattice constant, and the binding energy, respectively.

<b>Element</b>	<b>Function</b>	<b>a (Å)</b>	<b>c/a</b>	<b>E (eV/atom)</b>
<b>Zr (HCP)</b>	<b>Exp.[15]</b>	3.23	1.59	-6.25
	<b>DFT</b>	3.24	1.61	-5.61
	<b>Error (%)</b>	0.31	1.26	-10.24
<b>Ti (HCP)</b>	<b>Exp.[15]</b>	2.95	1.59	-4.85
	<b>DFT</b>	2.90	1.61	-4.38
	<b>Error (%)</b>	-1.69	1.26	-9.69
<b>Ta (BCC)</b>	<b>Exp.[15]</b>	3.3	-	-8.1
	<b>DFT</b>	3.29	-	-7.38
	<b>Error (%)</b>	-0.30	-	-8.89
<b>Si(DIA)</b>	<b>Exp.[15]</b>	5.43	-	-4.63
	<b>DFT</b>	5.47	-	-4.57
	<b>Error (%)</b>	0.74	-	-1.30

Table S3 The experimental and DFT calculation values (by CASTEP) of lattice constant, elastic constants ( $C_{11}$ ,  $C_{12}$ ,  $C_{13}$ ,  $C_{33}$ ,  $C_{44}$ ), bulk modulus (B) and shear modulus (S) for Ti, Zr, Ta and Si unit cells.

<i>Element</i>	<i>Property</i>	<i>Exp. [16, 24] (GPa)</i>	<i>DFT (GPa)</i>	<i>Error(%)</i>
Zr (HCP)	$C_{11}$	154.40	166.25	7.67
	$C_{12}$	67.20	57.52	-14.41
	$C_{13}$	64.60	68.71	6.36
	$C_{33}$	172.50	184.91	7.20
	$C_{44}$	36.30	19.38	-46.62
	Bulk modulus	97.10	100.19	3.18
	Shear modulus	42.20	40.12	-4.93
Ti (HCP)	$C_{11}$	176.10	175.38	-0.41
	$C_{12}$	86.80	86.36	-0.51
	$C_{13}$	68.30	70.75	3.59
	$C_{33}$	189.10	204.26	8.02
	$C_{44}$	50.80	46.30	-8.86
	Bulk modulus	109.8	112.82	2.75
	Shear modulus	50.4	49.04	-2.69
Ta (BCC)	$C_{11}$	264.00	267.57	1.35
	$C_{12}$	158.00	154.72	-2.07
	$C_{44}$	82.6	77.61	-6.04
	Bulk modulus	200.00	192.33	-3.80
	Shear modulus	69.00	69.13	0.18
Si(DIA)	$C_{11}$	165.70	156.09	-5.80
	$C_{12}$	63.90	56.17	-12.10
	$C_{44}$	79.60	79.81	0.27
	Bulk modulus	97.80	89.48	-8.51
	Shear modulus	76.90	67.87	-11.74

Table S4. The parameters of tight-binding potential for Zr-Zr, Zr-Ti, Zr-Ta, Ti-Ti, Ti-Ta, Ta-Ta, Ta-Si

<i>Type</i>	<i>A(eV)</i>	<i>ζ(eV)</i>	<i>p</i>	<i>q</i>	<i>r<sub>0</sub>(Å)</i>
<b><i>Zr-Zr</i></b>	0.162	2.095	10.727	2.257	3.138
<b><i>Zr-Ti</i></b>	0.120	1.684	8.984	1.598	3.040
<b><i>Zr-Ta</i></b>	0.265	2.632	7.342	1.371	3.034
<b><i>Ti-Ti</i></b>	0.094	1.406	11.880	2.118	2.849
<b><i>Ti-Ta</i></b>	0.246	2.325	7.999	1.836	2.889
<b><i>Ta-Ta</i></b>	0.299	2.571	7.702	1.870	2.859
<b><i>Ta-Si</i></b>	0.363	2.694	11.362	3.124	2.598

Table S5. The parameters of Tersoff potential for Si-Si, Si-Ti and Si-Zr

<i>Type</i>	<i>Si-Si</i>	<i>Zr-Si</i>	<i>Ti-Si</i>
<i>A(eV)</i>	7835.380	2251.660	3003.100
<i>B(eV)</i>	45.087	175.073	7.666
<i>λ</i>	3.851	2.603	3.418
<i>μ</i>	1.079	1.474	0.559
<i>β</i>	0.429	0.468E-05	2.300E-06
<i>n</i>	21.161	39.960	10.604
<i>c</i>	27340.700	4061.980	34231.700
<i>d</i>	119.344	3.252	7.797
<i>h</i>	-0.330	-0.062	-0.211
<i>R(Å)</i>	2.783	3.216	2.906
<i>S(Å)</i>	2.986	3.562	3.206

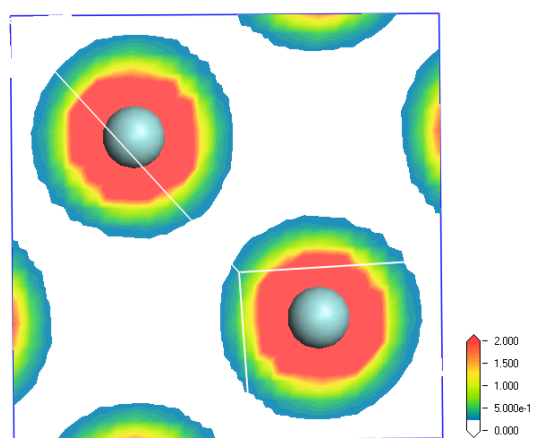
Table S6. Binding energy (E), Binding energy of one-atom-defect structure ( $E_d$ ), elastic constants ( $C_{11}$ - $C_{44}$ ) of all referenced configurations predicted by the DFT calculation and by the molecular statics (MS) based on potential functions with the best fitted parameters.

<i>Metal</i>	<i>Method</i>	<i>E(eV/atom)</i>	<i>E<sub>d</sub>(eV/atom)</i>	<i>C<sub>11</sub>(GPa)</i>	<i>C<sub>12</sub>(GPa)</i>	<i>C<sub>44</sub>(GPa)</i>
Zr	<i>DFT</i>	-5.61	-5.43	166.25	57.52	19.38
	<i>MS</i>	-5.89	-5.74	147.87	87.42	38.63
	<i>Error(%)</i>	4.99	5.71	-11.06	51.98	99.33
Ti	<i>DFT</i>	-4.38	-4.06	175.38	86.36	46.3
	<i>MS</i>	-4.21	-3.98	164.15	90.48	41.28
	<i>Error(%)</i>	-3.88	-1.97	-6.40	4.77	-10.84
Ta	<i>DFT</i>	-7.38	-6.28	267.57	154.72	77.61
	<i>MS</i>	-6.74	-6.53	137.05	132.95	78.23
	<i>Error(%)</i>	-8.67	3.98	-48.78	-14.07	0.80
Si	<i>DFT</i>	-4.57	-4.37	156.09	56.17	79.81
	<i>MS</i>	-4.45	-4.21	159.25	53.56	68.88
	<i>Error(%)</i>	-2.63	-3.66	2.02	-4.65	-13.70
<i>Alloy</i>	<i>Method</i>	<i>E(eV/atom)</i>	<i>E<sub>d</sub>(eV/atom)</i>	<i>C<sub>11</sub>(GPa)</i>	<i>C<sub>12</sub>(GPa)</i>	<i>C<sub>44</sub>(GPa)</i>
Zr <sub>1</sub> Ti <sub>1</sub>	<i>DFT</i>	-5.27	-4.94	125.37	84.82	43.50
	<i>MS</i>	-5.26	-4.90	191.66	51.90	57.48
	<i>Error(%)</i>	0.24	0.90	52.88	-38.81	32.14
Zr <sub>3</sub> Ti <sub>1</sub>	<i>DFT</i>	-5.39	-5.09	107.09	87.16	49.10
	<i>MS</i>	-5.62	-5.33	117.12	85.48	56.79
	<i>Error(%)</i>	-4.29	4.55	9.37	-1.93	15.66
Zr <sub>1</sub> Ti <sub>3</sub>	<i>DFT</i>	-5.20	-4.99	100.56	97.46	47.13
	<i>MS</i>	-4.82	-4.70	99.20	73.95	50.78
	<i>Error(%)</i>	7.41	5.78	-1.35	-24.12	7.74
Ti <sub>1</sub> Ta <sub>1</sub>	<i>DFT</i>	-5.86	-5.41	115.03	161.78	18.93
	<i>MS</i>	-5.94	-5.48	131.85	79.99	42.22
	<i>Error(%)</i>	1.44	1.35	14.62	-50.56	123.03
Ti <sub>3</sub> Ta <sub>1</sub>	<i>DFT</i>	-5.08	-4.44	113.61	139.63	77.99
	<i>MS</i>	-5.28	-4.65	134.35	97.36	63.78
	<i>Error(%)</i>	3.90	-4.69	18.26	-30.27	-18.22
Ti <sub>1</sub> Ta <sub>3</sub>	<i>DFT</i>	-6.57	-6.13	61.12	215.05	50.88

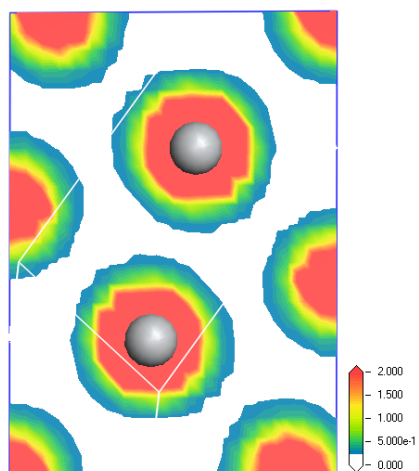
	<i>MS</i>	-6.35	-6.20	121.05	93.60	55.21		
	<i>Error</i>	-3.26	1.14	98.05	-56.48	8.51		
Zr <sub>1</sub> Ta <sub>1</sub>	<i>DFT</i>	-7.02	-6.98	168.18	123.49	5.25		
	<i>MS</i>	-7.41	-7.11	300.16	24.66	27.36		
	<i>Error(%)</i>	5.56	1.86	78.48	-80.03	421.14		
Zr <sub>3</sub> Ta <sub>1</sub>	<i>DFT</i>	-6.25	-6.21	89.67	122.65	55.20		
	<i>MS</i>	-6.96	-7.11	111.26	83.02	56.51		
	<i>Error(%)</i>	11.36	14.49	24.08	-32.31	2.37		
Zr <sub>1</sub> Ta <sub>3</sub>	<i>DFT</i>	-7.77	-7.37	71.43	196.40	44.16		
	<i>MS</i>	-7.30	-7.03	97.01	78.91	49.43		
	<i>Error(%)</i>	-6.05	-4.61	35.81	-59.82	11.93		
<i>Alloy</i>	<i>Method</i>	<i>E(eV/atom)</i>	<i>C<sub>11</sub>(GPa)</i>	<i>C<sub>12</sub>(GPa)</i>	<i>C<sub>13</sub>(GPa)</i>	<i>C<sub>22</sub>(GPa)</i>	<i>C<sub>33</sub>(GPa)</i>	<i>C<sub>44</sub>(GPa)</i>
ZrSi	<i>DFT</i>	-5.96	225.48	111.95	76.76	244.93	295.16	71.84
	<i>MS</i>	-6.41	203.76	131.46	121.02	226.91	245.83	70.65
	<i>Error(%)</i>	7.55	-9.63	17.43	57.66	-7.36	-16.71	-1.66
ZrSi <sub>2</sub>	<i>DFT</i>	-5.51	248.41	82.03	83.80	198.38	295.24	106.28
	<i>MS</i>	-5.20	260.50	108.23	102.05	142.71	285.51	108.70
	<i>Error(%)</i>	-5.63	4.87	31.94	21.78	-28.06	-3.30	2.28
Zr <sub>3</sub> Si <sub>2</sub>	<i>DFT</i>	-6.04	270.11	54.17	97.84	270.11	168.12	101.53
	<i>MS</i>	-6.80	212.55	117.20	115.23	212.55	188.12	90.19
	<i>Error(%)</i>	12.58	-21.31	116.36	17.77	-21.31	11.90	-11.17
TiSi	<i>DFT</i>	-5.17	211.78	118.36	73.64	254.24	296.56	85.87
	<i>MS</i>	-5.97	135.36	122.69	126.80	193.11	177.95	55.48
	<i>Error(%)</i>	15.47	-36.08	3.66	72.19	-24.04	-40.00	-35.39
TiSi <sub>2</sub>	<i>DFT</i>	-5.00	261.92	59.03	98.93	188.59	299.99	81.09
	<i>MS</i>	-5.19	204.97	79.66	155.20	107.00	212.23	73.54
	<i>Error(%)</i>	3.80	-21.74	34.95	56.88	-43.26	-29.25	-9.31
Ti <sub>3</sub> Si	<i>DFT</i>	-4.88	123.10	123.72	102.49	123.10	160.95	71.37
	<i>MS</i>	-5.64	139.38	109.65	79.49	139.38	170.70	31.49
	<i>Error(%)</i>	15.57	13.23	-11.37	-22.44	13.23	6.06	-55.88
Ta <sub>2</sub> Si	<i>DFT</i>	-6.95	318.96	147.72	158.45	318.96	278.54	112.73
	<i>MS</i>	-6.76	235.98	219.69	138.59	235.98	181.58	74.60
	<i>Error(%)</i>	-2.73	-26.02	48.72	-12.53	-26.02	-34.81	-33.82
Ta <sub>5</sub> Si <sub>3</sub>	<i>DFT</i>	-6.84	372.79	135.04	116.58	372.79	330.03	85.92
	<i>MS</i>	-6.24	305.09	184.47	106.38	305.09	190.89	12.41
	<i>Error(%)</i>	-8.77	-18.16	36.60	-8.75	-18.16	-42.16	-85.56

TaSi <sub>2</sub>	<i>DFT</i>	-5.88	343.79	72.97	77.45	343.79	441.84	136.22
	<i>MS</i>	-6.94	316.39	174.22	151.30	316.39	446.70	31.80
	<i>Error(%)</i>	18.03	-7.97	138.76	95.35	-7.97	1.10	-76.66

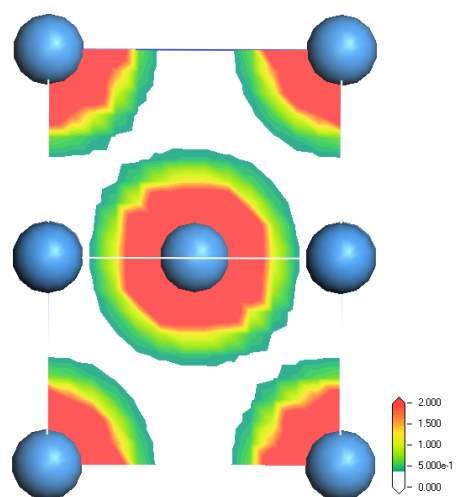
(a)Zr



(b)Ti



(c)Ta



(d)Si

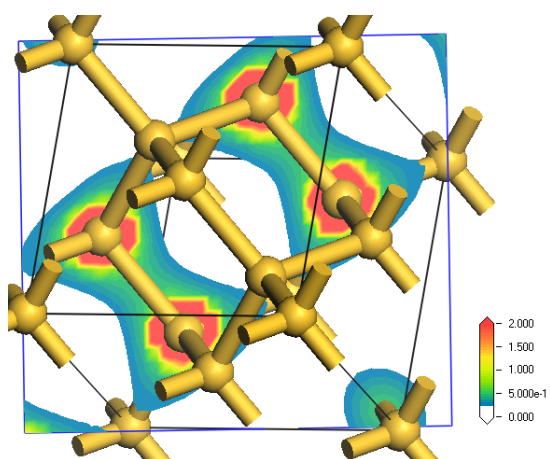
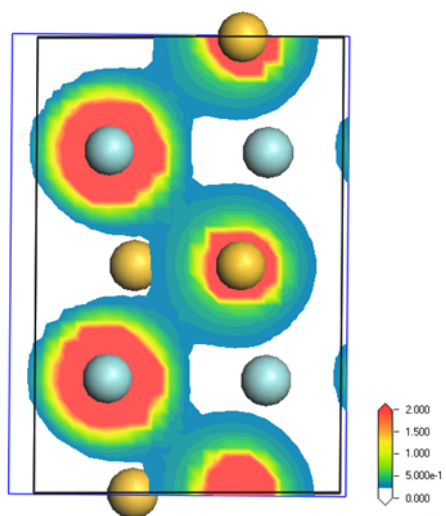
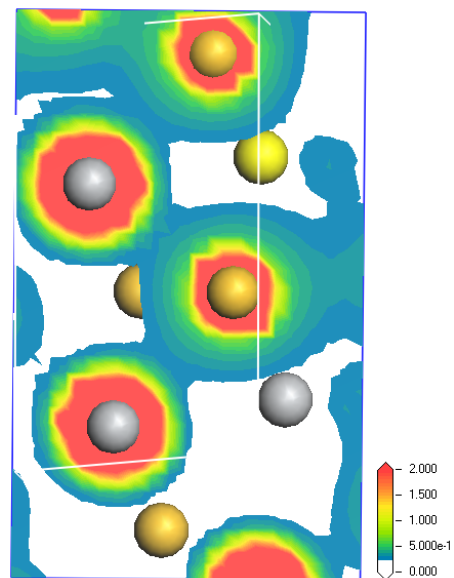


Fig. S1 Electron density distributions of (a) Zr (b) Ti (c) Ta (d) Si unit cells.

(a) ZrSi



(b) TiSi



(c) Ta<sub>5</sub>Si<sub>3</sub>

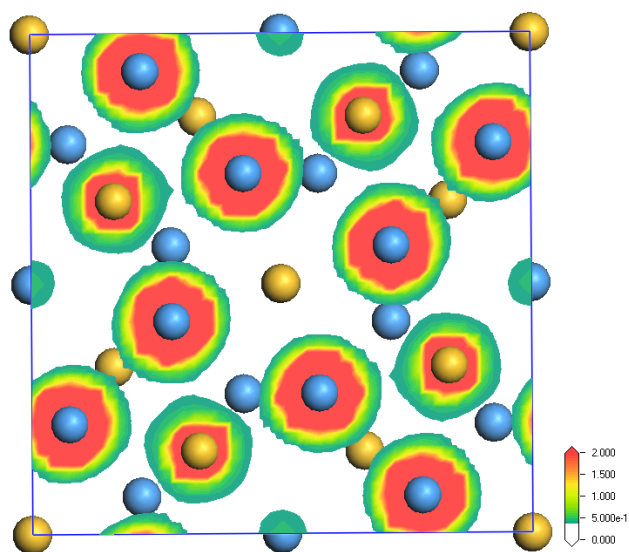


Fig. S2 Electron density distributions of (a) ZrSi (b) TiSi (c) Ta<sub>5</sub>Si<sub>3</sub> unit cells.

## Reference

- [1] G. Grochola, S. P. Russo, and I. K. Snook, "On fitting a gold embedded atom method potential using the force matching method," *The Journal of Chemical Physics*, vol. 123, p. 204719, 2005.
- [2] F. Ercolessi and J. B. Adams, "Interatomic Potentials from 1st-Principles Calculations - the Force-Matching Method," *Europhysics Letters*, vol. 26, pp. 583-588, Jun 10 1994.
- [3] O. Schob, F. Benesovsky, and H. Nowotny, "Strukturbestimmung an Einigen Phasen in Den Systemen - Zr-Al-Si Und Hf-Al-Si[ZrAl<sub>3</sub>(Si) - ZrSi(Al), Hf(Si,Al) - Zr<sub>3</sub>Si<sub>2</sub> - Hf<sub>3</sub>Si<sub>2</sub>]," *Monatshefte Fur Chemie*, vol. 92, pp. 1218-&, 1961.
- [4] A. Raman and K. Schubert, *Z Metallkd*, vol. 56, pp. 44-52, 1965.
- [5] M. Setton and J. Vanderspiegel, "STRUCTURAL AND ELECTRICAL-PROPERTIES OF ZRSI<sub>2</sub> AND ZR<sub>2</sub>CUSI<sub>4</sub> FORMED BY RAPID THERMAL-PROCESSING," *Journal of Applied Physics*, vol. 70, pp. 193-197, Jul 1991.
- [6] O. G. K. Y. A. Kocherzhinskii, Shishkin E.A., *Doklady Chemistry*, vol. 261, pp. 464-465, 1981.
- [7] I. Engström and B. Lönnberg, "Thermal expansion studies of the group IV-VII transition-metal disilicides," *Journal of Applied Physics*, vol. 63, pp. 4476-4484, 1988.
- [8] N. F. P. G. V. Samsonov, L.A. Dvorina, *Inorg. Mater.*, vol. 13, pp. 1429-1431, 1977.
- [9] J. Jongste, O. Loopstra, G. Janssen, and S. Radelaar, "Elastic constants and thermal expansion coefficient of metastable C<sub>49</sub> TiSi<sub>2</sub>," *Journal of Applied Physics*, vol. 73, pp. 2816-2820, 1993.
- [10] Y. A. K. V.N. Svechnikov, L.M. Yupko, O.G. Kulik, E.A. Shishkin, *Dokl. Chem. Technol.*, vol. 192, pp. 82-85, 1970.
- [11] S. D. Materials Studio distributed by Accelrys Software Inc., CA, USA.
- [12] M. D. Segall, P. J. D. Lindan, M. J. Probert, C. J. Pickard, P. J. Hasnip, S. J. Clark, and M. C. Payne, "First-principles simulation: ideas, illustrations and the CASTEP code," *Journal of Physics-Condensed Matter*, vol. 14, pp. 2717-2744, Mar 25 2002.
- [13] J. P. Perdew and Y. Wang, "Accurate and Simple Analytic Representation of the Electron-Gas Correlation-Energy," *Physical Review B*, vol. 45, pp. 13244-13249, Jun 15 1992.
- [14] B. Delley, "An All-Electron Numerical-Method for Solving the Local Density Functional for Polyatomic-Molecules," *Journal of Chemical Physics*, vol. 92, pp. 508-517, Jan 1 1990.
- [15] C. Kittel and P. McEuen, *Introduction to solid state physics* vol. 7: Wiley New

York, 1996.

- [16] M. A. Hopcroft, W. D. Nix, and T. W. Kenny, "What is the Young's Modulus of Silicon?," *Journal of Microelectromechanical Systems*, vol. 19, pp. 229-238, Apr 2010.
- [17] F. Cleri and V. Rosato, "Tight-Binding Potentials for Transition-Metals and Alloys," *Physical Review B*, vol. 48, pp. 22-33, Jul 1 1993.
- [18] B.-T. Wang, P. Zhang, H.-Y. Liu, W.-D. Li, and P. Zhang, "First-principles calculations of phase transition, elastic modulus, and superconductivity under pressure for zirconium," *Journal of Applied Physics*, vol. 109, p. 063514, 2011.
- [19] X. M. Tao, P. Jund, C. Colinet, and J. C. Tedenac, "Phase stability and physical properties of Ta<sub>5</sub>Si<sub>3</sub> compounds from first-principles calculations," *Physical Review B*, vol. 80, Sep 2009.
- [20] Y.-C. Wang and C.-Y. Wu, "Molecular dynamics simulation of Cu-Zr-Al metallic-glass films under indentation," *Thin Solid Films*, 2013.
- [21] V. Rosato, M. Guillope, and B. Legrand, "Thermodynamical and Structural-Properties of Fcc Transition-Metals Using a Simple Tight-Binding Model," *Philosophical Magazine a-Physics of Condensed Matter Structure Defects and Mechanical Properties*, vol. 59, pp. 321-336, Feb 1989.
- [22] P. J. Hsieh, Y. C. Lo, J. C. Huang, and S. P. Ju, "On the latest stage of transformation from nanocrystalline to amorphous phases during ARB: Simulation and experiment," *Intermetallics*, vol. 14, pp. 924-930, Aug-Sep 2006.
- [23] P. J. Hsieh, Y. C. Lo, C. T. Wang, J. C. Huang, and S. Ju, "Cyclic transformation between nanocrystalline and amorphous phases in Zr based intermetallic alloys during ARB," *Intermetallics*, vol. 15, pp. 644-651, May-Jun 2007.
- [24] M. A. Karolewski, "Tight-binding potentials for sputtering simulations with fcc and bcc metals," *Radiation Effects and Defects in Solids*, vol. 153, pp. 239-255, 2001.
- [25] G. Simmons, "Single crystal elastic constants and calculated aggregate properties," DTIC Document 1965.
- [26] J. Tersoff, "Modeling Solid-State Chemistry - Interatomic Potentials for Multicomponent Systems," *Physical Review B*, vol. 39, pp. 5566-5568, Mar 15 1989.
- [27] J. D. Gale, "GULP: A computer program for the symmetry-adapted simulation of solids," *Journal of the Chemical Society-Faraday Transactions*, vol. 93, pp. 629-637, Feb 21 1997.
- [28] S. Hamad, C. R. A. Catlow, S. M. Woodley, S. Lago, and J. A. Mejias, "Structure

and stability of small TiO<sub>2</sub> nanoparticles," *Journal of Physical Chemistry B*, vol. 109, pp. 15741-15748, Aug 25 2005.

- [29] D. J. Wales and J. P. K. Doye, "Global optimization by basin-hopping and the lowest energy structures of Lennard-Jones clusters containing up to 110 atoms," *Journal of Physical Chemistry A*, vol. 101, pp. 5111-5116, Jul 10 1997.